Low-Overhead Control Channels in Wireless Networks

Eugene Chai, *Member, IEEE,* and Kang G. Shin, *Fellow, IEEE*

Abstract—Low-latency, low-overhead and reliable control channels are essential to the efficient operation of wireless networks. However, control channels that utilize current in-band and out-of-band designs do not fully meet this requirement. In this paper, we design and implement Aileron, a novel control channel based on automatic modulation recognition that carries control frames over an OFDM(A) PHY by varying the modulation rate of the OFDM subcarriers. With Aileron, the control information is embedded into the *modulation type*, not as the actual symbol value. The thus-transmitted information can be received with little to no frame synchronization. We have evaluated Aileron using both extensive simulations and real-world measurements, and discovered that control frames can be transmitted with more than 80 percent accuracy using only 10 OFDM blocks on a channel with SNR of merely 10 dB. In order to demonstrate its applicability and efficiency in realistic networking scenarios, we also show how Aileron can be used in conjunction with a fine-grained channel access protocol to increase throughput under heterogeneous link conditions.

Index Terms—Wireless networks, control channels, low overhead

1 Introduction

Spectrum aggregation is necessary to achieve the high bandwidth channels needed to meet the coverage and capacity demands of mobile wireless devices in the face of growing spectrum scarcity. It is arguable that a single spectrum band can fully meet the demands from wireless users. For example, even though devices can achieve high throughput by using the 60 GHz bands, the high attenuation of millimeter wave transmissions limits the coverage at that frequency. Conversely, 2.4 GHz ISM bands offer good coverage but are hamstrung by the limited bandwidth availability. Furthermore, it is well-known that simply increasing the contiguous bandwidth within a specific spectrum band does not necessarily improve throughput due to increased interference [1]. Hence, even in widely-deployed distributed WiFi CSMA networks, spectrum aggregation must be employed to combine the coverage and capacity features from multiple disjoint spectrum bands.

Partially overlapping channels in dynamic spectrum networks. Current WiFi networks employ a small number of well-defined channels, with each channel defined by a known center frequency and bandwidth. All channels occupy only a continuous block of spectrum. On the other hand, a channel in a dynamic spectrum aggregation network is a logical construct built from multiple disjoint spectrum bands. The number of possible channels is thus exponentially larger—given N available spectrum bands, we can construct $N!$ possible channels. Furthermore, the number and location of available channels vary across different devices. Due to the large number of heterogeneously constructed logical channels, partially overlapping channels between multiple devices are common.

Coordination is the key challenge. Coordination and control, such as those carried over RTS/CTS frames, over current WiFi networks take place *coherently*. Coherent communication requires that the PHY of the receiver can decode frames in their entirety, so as to extract the control messages carried within them. This means that the transmitter and the receiver must share the same channel. In typical multi-carrier dynamic spectrum networks, coherent coordination is established via rendezvous protocols [2] or dedicated, predefined or dynamically negotiated [3] control channels. Such approaches incur a significant channel setup/changeover delay and thus, cannot be easily adapted for quickly changing channel conditions, such as those expected in highly mobile networks.

Our solution: Non-coherent control channel. In this paper, we design and implement Aileron, a novel low-overhead control channel built upon *non-coherent* communication techniques. Aileron encodes information using the *modulation rate* of individual OFDM subcarriers while the receiver uses *modulation identification* techniques to recover this information. With a non-coherent control channel, devices can receive control information even from partially overlapping channels. Devices can extract information from the set of subcarriers in the portion of the frame that it can receive, and can still extract control information from transmissions on partially overlapping channels.

Our key contribution with Aileron is the use of a *low-overhead* modulation identification technique for exchanging control information. Typical modulation identification techniques rely on a large amount of signal data and higher-order statistics [4], [5] to accurately decern the modulation of the transmitted signal. Such techniques thus incur a significant delay and processing overhead, and are unsuitable for use in data transmission. Aileron

- *E. Chai is with the Computer Science and Engineering Department, University of Michigan, 2260 Hayward Street, MI 08540.*
- *K. G. Shin is with the Electrical Engineering and Computer Science Department, University of Michigan, MI 48109.*

Manuscript received 15 Aug. 2012; revised 2 Sept. 2014; accepted 30 Nov. 2014. Date of publication 12 Jan. 2015; date of current version 29 Sept. 2015. For information on obtaining reprints of this article, please send e-mail to: reprints@ieee.org, and reference the Digital Object Identifier below. Digital Object Identifier no. 10.1109/TMC.2014.2384011

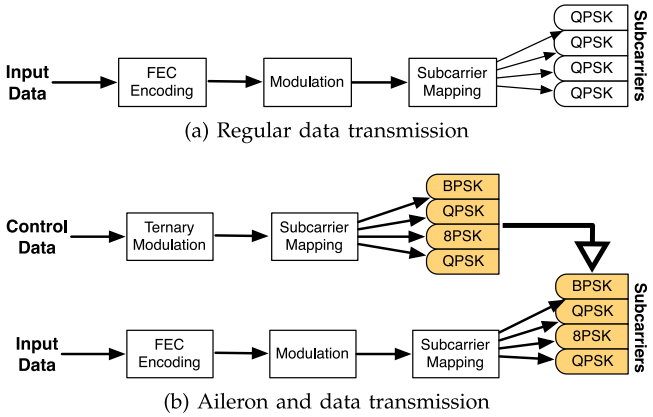

Fig. 1. Aileron encodes information using the modulation rate of the subcarriers. The frame data is then carried using the Aileron-defined rates.

employs a novel, computationally efficient, yet accurate modulation scheme (more than 99 percent accuracy) for exchanging information over partially overlapping bands.

Our contributions can be summarized as follows. First, we design a reliable, low-overhead modulation-based signaling scheme, Aileron. Second, we implement Aileron on a USRP2 platform and demonstrate, via experimentation, its efficiency and robustness. We also evaluate it under a wide range of channel conditions, demonstrating its superior performance under varying channel and mobility conditions. Third, we demonstrate how Aileron can be combined with a FICA-style frequency-domain contention scheme to enable frame aggregation in dynamic spectrum access networks.

The paper is organized as follows. We give an overview of Aileron in Section 2 and describe the key ideas and techniques behind modulation-based signaling in Sections 3 and 4. We then evaluate Aileron using simulations and real-world experiments in Sections 5 and 6, respectively. We briefly discuss other real-world concerns of Aileron in Section 7. To further motivate the benefits of Aileron in real-world networks, we demonstrate the ability of Aileron to enhance spectrum usage in Section 8. We discuss related work in Section 9 and conclude the paper in Section 10.

2 Overview of Aileron

Aileron operates in conjunction with OFDM transmissions and encodes information in the *modulation rate*, rather than the constellation point, as is the case with coherent transmissions.

2.1 How Does Aileron Work?

Aileron overlays a low bitrate control channel on top of OFDM frames: data is packed into the subcarriers of the OFDM frame by the PHY protocol, while the control information is encoded using the *modulation rate* of these data subcarriers. Aileron uses three modulation rates for encoding data: BPSK, QPSK and 8PSK.

Consider the case where data is transmitted using an OFDM frame, as shown in Fig. 1a. In current WiFi networks, the data to be transmitted is first run through an FEC encoder, followed by an interleaver and modulator. The modulation rate used here is assumed to be either

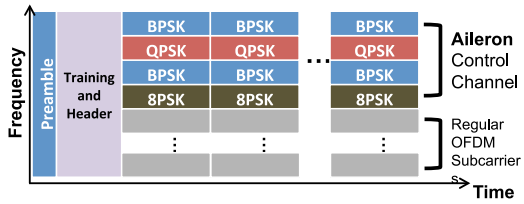

Fig. 2. Aileron only occupies part of the transmitted frame.

determined by an auto-rate algorithm or fixed beforehand. Finally, the modulated data is mapped to multiple OFDM subcarriers.

Aileron transmits control information together with the data bits, as shown in Fig. 1b. To see how this works, consider an example case where BPSK, QPSK, and 8PSK are mapped to values 0, 1, and 2, respectively. A transmitter that needs to send an integer-valued control frame first converts control message into ternary numbers. The modulation rate of each subcarrier in the Aileron control channel is then set according to the value of its corresponding ternary digit. This subcarrier modulation layout is then used to carry the original frame information. At the receiver, the control frame is recovered by recognizing the modulation rate of each subcarrier and reconstructing the corresponding ternary number. Note that no CSMA overhead is incurred for the control frames transmitted by Aileron.

2.2 How is Aileron Integrated into Data Networks?

Fig. 2 shows how Aileron is integrated into a data frame. Aileron is only used on a fraction of the subcarriers in a frame. The bandwidth of the control channel is directly proportional to the number of subcarriers used by Aileron. Note that the choice of subcarriers affects the set of partially overlapping channels that can receive the Aileron control message. In order to maximize the reachability of this control channel, Aileron can use several disjoint sets of subcarriers.

The Aileron control channel only needs to be employed when there are control messages to be sent. Regular OFDM modulation rates can be used for all subcarriers if the frame does not carry any control message.

Our experimentation with Aileron over real-world channels has shown that

- over good quality channels (25 dB median SNR), Aileron can detect BPSK, QPSK and 8PSK with accuracy of 100, 98 and 86 percent, respectively,
- over intermediate quality channels (18 dB median SNR), the accuracy of Aileron is 80, 82 and 89 percent, respectively,
- over poor quality channels (7 dB median SNR), the accuracy of Aileron is very poor.

Hence, we integrate Aileron with existing networks as follows.

Aileron is used on subcarriers with higher SNR. This ensures that the accuracy of Aileron is as high as possible. Note that due to the frequency selectivity of wide-band channels, even channels with low effective SNR have multiple subcarriers with high SNR [6]. These subcarriers are found using the CSI, and are used for Aileron control channels.

Number of Aileron modulation rates used depends on required accuracy. Since Aileron uses non-coherent signaling, the

detection accuracy of each Aileron modulation rate is different. Hence, the number of modulation rates used by Aileron must be adjusted to match the desired accuracy of the control channel. We note that control information does not necessarily need to be transmitted with 100 percent accuracy. For example, if a WiFi device fails to decode an RTS/CTS frame correctly, energy sensing and exponential backoff will still be able to limit channel interference, albeit with lower efficiency. Under high SNR channels, if high control channel accuracy is required, Aileron will be limited to using only BPSK and QPSK for signaling. Otherwise, all three modulation rates will be employed.

2.3 How Does an Aileron Receiver Know if a Frame Contains an Aileron Control Channel?

Recall that Aileron results in varying modulation rates across different subcarriers, while typical WiFi transmissions use a single modulation rate for all subcarriers. Aileron receiver decodes Aileron control messages by detecting the modulation rate used in each subcarrier. The Aileron receiver determines that a control message is present in the frame if it detects a variation of modulation rates across multiple subcarriers. Otherwise, it simply ignores the frame.

2.4 How Does a Non-Aileron Receiver Decode the Aileron Frame?

A non-Aileron receiver that shares the same channel as the transmitter can decode the frame coherently. The header will carry additional bits to specify the modulation rates of each of the Aileron subcarriers and a non-Aileron receiver demodulates the Aileron subcarriers according to the indicated rates. Other non-Aileron subcarriers can be demodulated according to the pre-determined auto-rate modulation rate.

2.5 What is the Overhead of Aileron on the Network Throughput?

Synchronization overhead is low. Aileron can acquire OFDM symbols on a symbol-by-symbol basis, as described in Section 4.1. Hence, no frame synchronization (that is typically achieved using preambles) is needed.

Overhead of additional header bits is small. Since 2 bits per subcarrier is enough to specify the rate of each subcarrier, the overall overhead will be small—even if all 64 subcarriers in a WiFi channel is used, only $64 \times 2/8 = 16$ additional bytes are required. There is merely 1 percent of the size of a typical 1.5 KB WiFi frame.

Overhead of Aileron modulation is negligible. Aileron may result in sub-optimal transmission rates as it can use modulation rates that are lower than the maximum supported by the channel. However, using Aileron in high-bandwidth WiFi networks is still more efficient than relying solely on coherent control signaling. This is because Aileron enables *simultaneous* transmission of both data and control messages to non-coherent receivers.

To understand the source of this efficiency, consider the transmission of a typical WiFi frame, as shown in Fig. 3. The total time taken to transmit a frame and receive an ACK is given by $(206 + T)\,\mu s$ where T is the actual airtime of the frame data. At MCS 31 (i.e., the highest 802.11n transmission rate), $T = 20\ \mu s$, thus resulting in a total airtime of $226\ \mu s$. If Aileron uses only BPSK, rather than the 64 QAM allowed at MCS 31, then this airtime increases to $326\ \mu s$—a 44 percent increase. However, recall that this additional time is used to transmit both the data *and* control message *simultaneously*. If coherent transmission is employed, the transmitter will first have to synchronize to the control channel, transmit the control frame and wait for the ACK, leading to an almost 100 percent increase in airtime over the standard WiFi transmission in Fig. 3. Hence, ***using Aileron in WiFi networks can more than halve the overhead of control frames***.

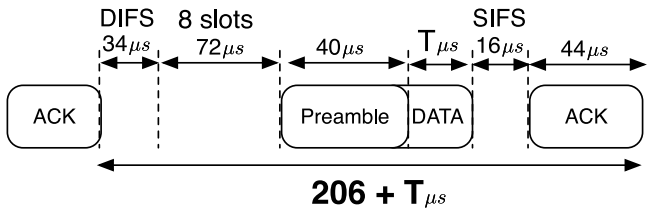

Fig. 3. Airtime of different components of a WiFi transmission.

We emphasize that this gain comes from our novel and unique use of coherent and non-coherent communications in wireless networks.

Aileron and 802.11n frame aggregation 802.11n frame aggregation increases the amount of data that is transmitted in each frame. In order to minimize the impact of Aileron, only the first frame is encoded using Aileron. The other frames will be transmitted without any Aileron overlay.

2.6 Aileron for Channel Monitoring

Contention management is a key in maximizing the capacity of current WiFi networks [7], [8], and accurate determination of transmission rate across multiple links is a key step to achieve this. In current WiFi networks, this is solely accomplished via *coherent* information exchange: nodes decode overheard frames to determine parameters such as the achievable rates of neighboring links, the contention behavior of hidden/exposed nodes, etc. Such coherent monitoring is difficult in networks with the prevalence of partially overlapping channels.

An Aileron device can still extract rate information from neighboring *non-Aileron* devices by detecting the modulation rate used in their transmissions. Furthermore, this can be accomplished without full knowledge of the spectrum fragments that constitute the logical channel. For example, Aileron can be used to construct CMAPs [7] even in partially overlapping channels without channel synchronization. Hence, Aileron is an important and effective vehicle even when used with non-Aileron devices.

3 Aileron Design

Aileron can operate in either active or passive modes. In both of these modes, control information is encoded in terms of the modulation rate of each subcarrier of transmitted data.

Fig. 4 shows the five constellations recognized by Aileron: BPSK, QPSK, 8 PSK, 16 QAM, and 64 QAM. Each point in a constellation diagram is used to encode $\log_2 M$ bits, where M is the total number of points in the diagram. For

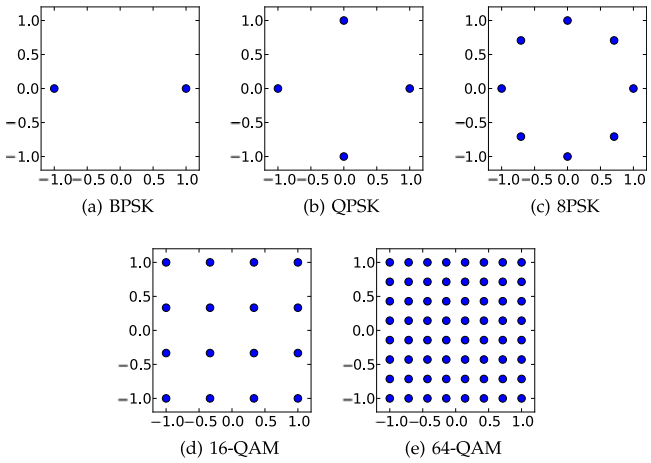

Fig. 4. Phase-Shift Keying (PSK) and Quadrature Amplitude Modulation (QAM) constellations recognized by Aileron.

an arbitrary subcarrier, the constellation diagram chosen to encode its bits determines its modulation rate. The PSK and QAM constellations in Fig. 4 are each chosen such that lower-level modulations are subsets of higher-level modulations—the QPSK constellation includes the two points of the BPSK constellation, and likewise, the 8 PSK constellation contains the points in both QPSK and BPSK. QAM constellations differ from the PSK constellations in that no constellation point exists along the in-phase and quadrature-phase axes. However, QAM constellations still maintain the subset property, although no QAM constellations are subsets of any PSK constellation, and vice versa.

3.1 Active-Mode Aileron

Fig. 5 illustrates the architecture of the Aileron transmitter and receiver of a simple three-node network. The transmitter, node A, contains an Aileron encoder module that maps the control frame into the modulation rates of the *Aileron subcarriers*. The modulation rates of these subcarriers are limited to BPSK, QPSK and 8 PSK, which correspond to the ternary bases, 0, 1 and 2. Subcarriers that are not used for

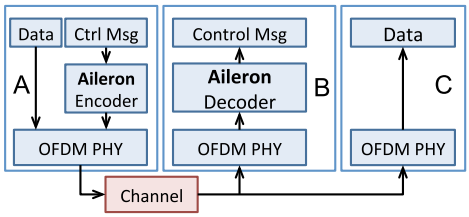

(a) Active-mode. A is an Aileron-enabled (WLAN) transmitter while C is an unmodified (WLAN) receiver.

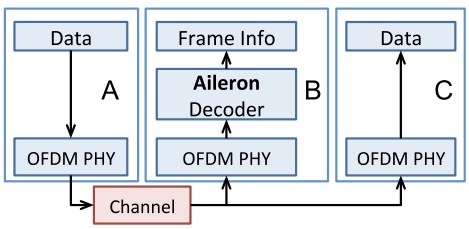

(b) Passive-mode. A and C are unmodified (WLAN) devices while B is an Aileron node.

Fig. 5. Active and passive Aileron.

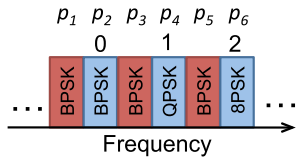

Fig. 6. Active-mode Aileron used to encode the value 5_{10} that is equal to 012_3.

Aileron signaling (i.e., non-Aileron-subcarriers) are not restricted to these constellations. Additionally, the subcarrier that precedes the Aileron subcarrier must be forced to the BPSK modulation. This is done to accommodate the OFDM symbol acquisition algorithm of Aileron as detailed in Section 4. The OFDM PHY at A uses these selected modulation rates to generate the OFDM frame that it transmits to C. The Aileron decoder at B recovers the control frame from the symbols received by the OFDM PHY from a multi-channel or partially-overlapping transmission.

For example, Fig. 6 shows a set of six consecutive OFDM subcarriers from a single 802.11g OFDM symbol, $p_1, \ldots, p_6$, that are used to represent a ternary value, with p_1 being the least significant ternary digit. Suppose that BPSK, QPSK and 8PSK map to integers 0, 1 and 2, respectively. In order to encode the base-10 number 5_{10} to 012_3, we set the non-Aileron-subcarriers p_1, p_3 and p_5 to be BPSK-modulated, and set the Aileron-subcarriers p_2, p_4 and p_6 to be BPSK, QPSK, and 8 PSK-modulated, respectively.

3.2 Passive-Mode Aileron

Rate-control algorithms in wireless networks select the fastest modulation rate given channel conditions. Hence, the state of the channel between a pair of communicating nodes can be inferred from the modulation rate used by them. For example, this information can be integrated into CMAPs [7] to increase the spatial reuse of more challenging whitespace and multi-channel networks.

Passive-mode Aileron does precisely this, identifying the modulation rate of each subcarrier of an unmodified OFDM frame. Fig. 5b shows an example Aileron device B that can overhear transmission between two non-Aileron devices A and C. A transmits frames to C using a standard 802.11a/g/n protocol and the Aileron decoder in B identifies the subcarrier modulation rates from the overheard OFDM symbols recovered by the PHY. Aileron can differentiate between BPSK, QPSK and 8 PSK. It can also differentiate between PSK and QAM, but the identification of 16 and 64 QAM is more involved and the subject of our future work.

3.3 Automatic Modulation Recognition

In both passive and active Aileron, the Aileron decoder employs a novel algorithm for Automatic Modulation Recognition (AMR) [9] to determine the modulation type of each subcarrier in a group of N identically-modulated OFDM symbols. Let $S_k = \{s_{k,1}, \ldots, s_{k,N}\}$ be a sequence of received samples of the kth subcarrier of N consecutive OFDM symbols. These samples are modulated using a constellation $C = \{c_1, \ldots, c_M\}$ with M points. These OFDM symbols must satisfy:

$$\rho(s_{k,i}) = \rho(s_{k,j}),\ i \neq j,\ 1 \leq i, j \leq N,\ 1 \leq k \leq K. \quad (1)$$

where $\rho(s_{k,n})$ is the modulation rate of $s_{k,n}$ and K is the total number of subcarriers in each OFDM symbol. Note that it is possible for $\rho(s_{k,n}) \neq \rho(s_{k',n})$ when $k \neq k'$. How to differentiate between these modulations is described in Algorithm 1. Each of the modulation rates—BPSK, QPSK and 8 PSK—has an associated decision rule, indicated by the functions `is_bpsk`, `is_qpsk` and `is_8psk`, respectively. Active-mode Aileron only uses BPSK, QPSK and 8 PSK: it matches the signal samples against the BPSK and QPSK rules. If the samples match neither of these rules, the modulation is declared to be 8 PSK. Passive-mode Aileron matches the signal against all three rules and if no match is found, the modulation of samples is declared to be "QAM. Passive-mode Aileron does not differentiate between 16 and 64 QAM because the constellation points of QAM are encoded using both magnitude and phase. It is not possible to accurately recover the magnitude without proper calibration using the frame preamble. On the other hand, because it is easy to differentiate between the three PSK schemes, we will restrict the allowable modulation schemes in active-mode Aileron to the PSK modulations to improve signaling reliability.

Algorithm 1. Automatic Modulation Recognition

Data: S_k is a sequence of N constellation points
Result: Identified modulation
begin
  if `is_bpsk` S_k **then**
    return "BPSK";
  else if `is_qpsk` S_k **then**
    return "QPSK";
  else if *Active-mode* ***or*** `is_8psk` S_k **then**
    return " 8PSK";
  else
    return "QAM";
  end
end

4 Aileron Algorithm Details

4.1 How Does Aileron Acquire an OFDM Symbol?

Aileron identifies subcarrier modulation rates from the OFDM symbols that are recovered from arbitrary locations of the transmitted frame. Aileron differs from traditional communication protocols in that it operates on individual OFDM *symbols* rather than *frames*. Energy detection is used to determine the presence of a frame transmission. Note that energy detection will work even over partially overlapping channels. Once Aileron detects the frame, it corrects the frequency drifts and timing offsets before identifying the modulation rates of each subcarrier.

Symbol detection and frequency drift correction are performed together using the van de Beek ML estimation algorithm [10]. However, this algorithm still cannot always guarantee perfect timing recovery. This timing recovery error induces a phase error in the subcarriers, due to the known property of Discrete Fourier Transforms: a timing offset of l samples introduces a phase error of $e^{-j2\pi kl/M}$ in the kth subcarrier. The corrected symbol Y_k in the kth subcarrier is obtained using the relation:

$$Y_k = X_k \cdot X_{k-1}^*/|X_{k-1}| \tag{2}$$

where the $(\cdot)^*$ operator denotes the complex conjugate and X_k is the uncorrected symbol in the kth subcarrier. If the symbols X_k and X_{k-1} are from the same constellation, then this correction will preserve the modulation scheme for subsequent recognition by Aileron. For example, if X_k and X_{k-1} are modulated using QPSK, then Y_k will definitely be one of the QPSK constellation points. However, the actual constellation point held by X_k is lost, thus preventing the original bit content from being recovered. This does not affect Aileron since only the modulation type is of our interest.

In Aileron, if X_k is used to encode a bit of control information, then the modulation rate of X_{k-1} is set to BPSK to maximize the probability of correctly identifying the modulation type of X_k.

4.2 What Are the Decision Rules?

Consider a sequence of subcarrier values, S_k, modulated with C. The normalized mean squared error (MSE) between S_k and the ideal constellation points is

$$\mathrm{MSE}_C(S_k) = \frac{1}{N}\sum_{n=1}^{N}\left(\min_{c_m \in C}\left\{\frac{s_{k,n}}{|s_{k,n}|} - \frac{c_m}{|c_m|}\right\}\right)^2. \tag{3}$$

The normalization of S_k and C minimizes the errors due to the randomly varying magnitude of the received samples. The decision rule for each modulation scheme is based on the *difference* between the MSE of S_k to the constellations:

$$\Gamma_{C_1,C_2}(S_k) \triangleq \mathrm{MSE}_{C_1}(S_k) - \mathrm{MSE}_{C_2}(S_k). \tag{4}$$

To understand the intuition behind this rule, consider, as an example, the process of detecting a QPSK transmission. The MSE w.r.t. a BPSK constellation is larger than that w.r.t. an 8 PSK constellation, since there are more points in the 8 PSK constellation with which the QPSK transmission can be "matched" with. We note that with each modulation rate, the set of MSE differences with respect to different constellations can serve as its signature. Aileron uses these signatures to identify the modulation rate in each subcarrier.

Fig. 7 illustrates the signatures of different modulation rates under varying SNR. We show the mean and standard deviation of the difference in MSE of the received symbols of each supported modulation scheme with respect to the ideal constellations. For every supported modulation, we transmit 320 symbols using 10 OFDM blocks of 32 subcarriers each over an AWGN channel with varying SNR levels. In each figure, we use the notation "$C_1 - C_2$" to represent $\Gamma_{C_1,C_2}(S_k)$.

a) Recognizing BPSK. The decision rule used to recognize received symbols that are modulated with BPSK is

$$\Gamma_{16\mathrm{QAM},64\mathrm{QAM}}(S_k) \geq \Gamma_{\mathrm{BPSK},\mathrm{QPSK}}(S_k), \quad \text{and} \tag{5}$$

$$\Gamma_{16\mathrm{QAM},64\mathrm{QAM}}(S_k) \geq \Gamma_{\mathrm{QPSK},8\mathrm{PSK}}(S_k), \quad \text{and} \tag{6}$$

$$\Gamma_{16\mathrm{QAM},64\mathrm{QAM}}(S_k) \geq \Gamma_{8\mathrm{PSK},16\mathrm{QAM}}(S_k). \tag{7}$$

By comparing Fig. 7a with the other sub-figures in Fig. 7, one of the defining characteristics of the BPSK modulation is found to be the fact that the mean value of $\mathrm{MSE}_{16\mathrm{QAM}}(S_k)-$

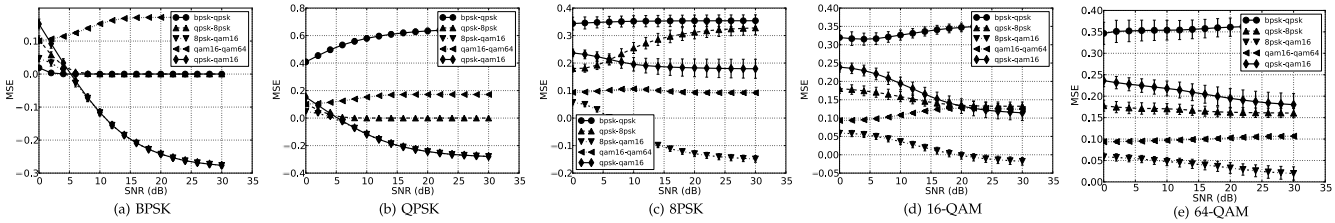

Fig. 7. Differences in MSE values for input sequences of different modulation rates.

$\mathrm{MSE}_{64\mathrm{QAM}}(S_k)$ is greater than all other MSE differences at SNRs greater than 2 dB. This is precisely the characteristic used in Eqs. (5), (6) and (7) to identify BPSK.

b) Recognizing QPSK. The decision rule to recognize an input stream modulated with QPSK is

$$\begin{aligned}\Gamma_{\mathrm{BPSK,QPSK}}(S_k) &\geq \Gamma_{\mathrm{16QAM,64QAM}}(S_k)\\ &\geq \Gamma_{\mathrm{QPSK,8PSK}}(S_k), \quad \text{and}\end{aligned} \tag{8}$$

$$\Gamma_{\mathrm{16QAM,64QAM}}(S_k) \geq \Gamma_{\mathrm{8PSK,16QAM}}(S_k). \tag{9}$$

The input symbols are first matched against the BPSK decision rule and the QPSK decision rule is considered only if the BPSK decision rule does not evaluate to be true on the sequence of input symbols. Fig. 7b shows the differences in MSE values of a QPSK input sequence with respect to the various ideal constellations. Obviously, the ideal BPSK constellation only contains half the points of the QPSK constellation. Hence, the mean distance between the QPSK input symbols to BPSK constellation points is significantly larger than the distance to the QPSK constellation points, thus making the QPSK constellation a "better" match for the input symbols than the BPSK constellation. As a result, we now have the properties

$$\Gamma_{\mathrm{BPSK,QPSK}}(S_k) \geq \Gamma_{\mathrm{QPSK,8PSK}}(S_k), \quad \text{and} \tag{10}$$

$$\Gamma_{\mathrm{BPSK,QPSK}}(S_k) \geq \Gamma_{\mathrm{16QAM,64QAM}}(S_k) \tag{11}$$

that hold true for expected MSE values. Since the mean distance of the QPSK- and BPSK-modulated received symbols to the other constellations is largely similar, Eqs. (6) and (7) still hold. Hence, we obtain the QPSK decision rule by combining Eqs. (6), (7), (10), and (11).

c) Recognizing 8 PSK. The decision rule to recognize a sequence of input symbols modulated using 8 PSK is

$$\Gamma_{\mathrm{QPSK,8PSK}}(S_k) \geq \Gamma_{\mathrm{QPSK,16QAM}}(S_k), \quad \text{and} \tag{12}$$

$$\Gamma_{\mathrm{QPSK,16QAM}}(S_k) \geq \Gamma_{\mathrm{16QAM,64QAM}}(S_k), \quad \text{and} \tag{13}$$

$$\Gamma_{\mathrm{QPSK,16QAM}}(S_k) < 0, \quad \text{and} \tag{14}$$

$$|\Gamma_{\mathrm{8PSK,16QAM}}(S_k)| \geq \alpha, \quad \text{and} \tag{15}$$

$$|\Gamma_{\mathrm{QPSK,8PSK}}(S_k) - \Gamma_{\mathrm{16QAM,64QAM}}(S_k)| \geq \beta. \tag{16}$$

The 8 PSK decision rule is used after both the BPSK and QPSK decision rules have been evaluated to be false on the input symbols. Hence, the 8 PSK decision rule only needs to differentiate 8 PSK from 16 and 64 QAM constellations. It is obvious from Figs. 7c, 7d and 7e that at SNRs greater than 6 dB, Eqs. (12)–(14) represent the key characteristics of the mean MSE differences that distinguish 8 PSK from 16 and 64 QAM. However, we also observe that with a 16 QAM-modulated input sequence (Fig. 7d), at SNRs greater than 18 dB, the mean values of $\mathrm{MSE}_{\mathrm{QPSK}}(S) - \mathrm{MSE}_{\mathrm{8PSK}}(S_k)$, $\mathrm{MSE}_{\mathrm{QPSK}}(S_k) - \mathrm{MSE}_{\mathrm{16QAM}}(S_k)$ and $\mathrm{MSE}_{\mathrm{16QAM}}(S_k) - \mathrm{MSE}_{\mathrm{64QAM}}(S_k)$ are close enough such that Eqs. (12)–(14) will hold true for a significant proportion of the actual MSE difference values, thus increasing the probability that 16 QAM will be mis-recognized as 8 PSK. To prevent this, Eqs. (15) and (16) ensure that these MSE differences must not be "too close" in order for the 8 PSK modulation to be correctly identified, with the degree of closeness to be defined by the parameters α and β. In our evaluation, we have found that $\alpha = \beta = 0.03$ gives the highest accuracy in differentiating 8 PSK from QAM constellations.

4.3 What is the Appropriate Size of N?

The variance of the MSE and the corresponding accuracy of Aileron depends on the length (N) of the input sequence S_k—AMR accuracy improves with longer input sequences but at the cost of a longer recognition delay.

The *AMR window* refers to the number of OFDM symbols used by each iteration of the AMR algorithm. This directly affects the length (N) of the sequence of input symbols S_k to the MSE equation (3). With active-mode Aileron, since every signaling subcarrier can use a different modulation scheme, an AMR window of length N (i.e., N OFDM blocks) will only produce N input symbols from a single subcarrier position. On the other hand, with passive-mode Aileron, all the data subcarriers use the same modulation scheme, so an AMR window of length N will contain $N \cdot K$ input symbols, where K is the number of data subcarriers per OFDM symbol. Our evaluation of Aileron will investigate the effects of the AMR window length on its accuracy.

5 Evaluation Using Simulated Channels

In this section, we evaluate the accuracy of Aileron under a wide range of simulated channel conditions. Some of these conditions, such as the doppler frequency seen at 100 m/s, cannot be easily created on a testbed. Thus, we use simulated channels to conduct a thorough evaluation of Aileron.

5.1 Experimental Setup

We implemented Aileron using an OFDMA PHY in GNURadio with the parameters listed in Table 1. We assume that Aileron is used in conjunction with a MAC protocol to coordinate channel access between transmitters. Hence, a single transmitter–receiver pair is sufficient to understand the

TABLE 1
Parameters Used in the OFDMA PHY

PHY Parameter	Value
Center frequency	2.4 GHz
Total bandwidth	12.5 MHz
Total subcarriers	1,024
Cyclic prefix length	256
No. of subchannels	16
No. of subcarriers per subchannel	64
No. of active-mode signaling subcarriers per subchannel	6
No. of guard subcarriers per subchannel	32

TABLE 2
Parameters Used in the Simulated Channels

Emulation Parameter	Value
Channel Model	`jtcInResC`, `jtcInOffC`, `jtcInComC` and `jtcOutUrbHRLAC`
Doppler Frequency	0-800 Hz in 80 Hz increments
Signal-to-Noise Ratio	0-30 dB in 2 dB increments
Modulation Rates	BPSK, QPSK, 8 PSK, 16 and 64 QAM
AMR Window	10, 15, 20, 25, 50, 75 and 100

The names of the channel model correspond to those used by MATLAB.

performance of Aileron. The transmitted samples are filtered using a simulated channel in MATLAB, using the parameters in Table 2, before being passed to the receiver.

Aileron is evaluated using the following JTC channel models in MATLAB: `jtcInResC`, `jtcInOffC`, `jtcInComC`, and `jtcOutUrbHRLAC` that correspond to Indoor residential C, Indoor office C, Indoor commercial C, and Outdoor urban high-rise areas–Low antenna C, respectively. Note that the variation of the doppler frequency from 0 to 800 in 80 Hz increments correspond to movement speeds of 0 to 100 m/s in increments of 10 m/s at a center frequency 2.4 GHz. The set of chosen channel models, doppler frequencies and SNRs represent a wide range of possible channel conditions under which the AMR algorithm has to operate. The SNR of the channel is representative of the interference seen on the channel. Due to space limitation, we will only present the evaluation results obtained using the `jtcInOffC` channel. The performances of Aileron under the other channel models are very similar.

5.2 Aileron Accuracy in Static Environments

Active-mode Aileron accuracy under different SNRs. Fig. 8 shows the accuracy of active-mode Aileron over channels without mobility: symbols are sent over the fading channel with no doppler shift, which is representative of a typical indoor office WLAN environment. This accuracy of Aileron is computed over 50,000 AMR windows of 10 OFDM symbols each.

Aileron is shown to be able to recognize BPSK and QPSK modulations with practically perfect accuracy at SNR above 16 dB. 8 PSK is detected correctly approximately 79 percent of the time at all SNR levels. It must be stressed that this level of accuracy is achieved using only

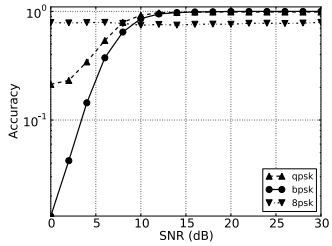

Fig. 8. Accuracy of active-mode Aileron over a simulated channel with no doppler shift and an AMR window of 10.

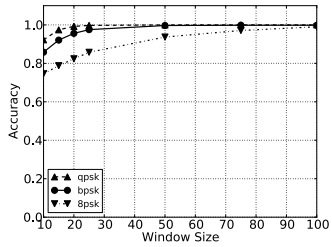

Fig. 9. Accuracy of active-mode Aileron with different AMR window sizes, no doppler shift and a SNR of 10 dB.

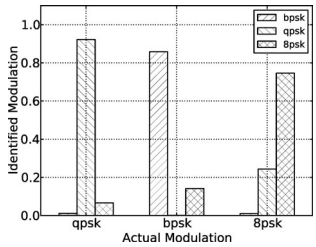

Fig. 10. Modulation detection profile with an AMR window of 10, a SNR of 10 dB and no doppler shift.

10 received symbols. As expected, the active-mode Aileron detection accuracy improves as we increase the number of symbols used by the AMR.

Active-mode Aileron accuracy under different AMR window sizes. Fig. 9 shows the AMR accuracy of active-mode Aileron when channel SNR and doppler shift are fixed at 8 dB and 0Hz, respectively. BPSK and QPSK modulations are recognized with 99 percent accuracy with 25 received symbols while 75 received symbols are required to achieve the same accuracy with 8 PSK. This trend—where 8 PSK is recognized less accurately than BPSK and QPSK, given the same number of received symbols—persists even at higher SNR levels.

Active-mode (mis)detection performance. Fig. 10 shows the detection probability of the all the possible modulation schemes that can be used in active-mode Aileron. BPSK and QPSK can be easily distinguished from each other but when the received symbols are modulated using 8 PSK, approximately 22 percent of the symbols are mis-recognized as QPSK. This error is due to the increased variance in the MSE differences used by the detection rules that is brought about by the multipath fading channel.

Passive-mode Aileron accuracy. Fig. 11 shows the accuracy of passive-mode Aileron when applied to data subcarriers

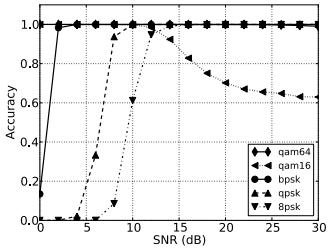

Fig. 11. Passive-mode Aileron accuracy in a simulated channel with no doppler shift and an AMR window of size 10.

from a single OFDMA subchannel. Since there are 32 data subcarriers in each OFDMA subchannel, 10 OFDM blocks will give 320 data symbols—significantly more than that obtained from the active-mode Aileron. The larger number of received data symbols increases the accuracy of Aileron: BPSK modulation is recognized with accuracy 100 percent of the time at SNRs greater than 2 dB while perfect identification of QPSK and 8 PSK occurs at SNRs above 10 and 16 dB, respectively. The AMR algorithm can always differentiate between the PSK modulations: mis-identified QPSK and 8 PSK modulations are always labeled as QAM, rather than another PSK scheme.

For the QAM schemes, 64 QAM is accurately identified at all SNR levels while 16 QAM is correctly identified only up to 12 dB, above which the recognition accuracy of 16 QAM encounters a significant drop as it is consistently mis-identified as QPSK. This is because at higher SNRs, the mean value of $\mathrm{MSE}_{\mathrm{QPSK}}(S) - \mathrm{MSE}_{\mathrm{8PSK}}(S)$, $\mathrm{MSE}_{\mathrm{QPSK}}(S) - \mathrm{MSE}_{\mathrm{16QAM}}(S)$ and $\mathrm{MSE}_{\mathrm{16QAM}}(S) - \mathrm{MSE}_{\mathrm{64QAM}}(S)$ of a 16 QAM-modulated input converges, as seen in Fig. 7d. With an AMR window size of 10 OFDM blocks, the variance of MSE differences is large enough for 16 QAM to be mistaken for QPSK with a high probability. If we double the input AMR window size to 20 blocks, 16 QAM will be identified with perfect accuracy, as shown in Fig. 12.

5.3 Aileron Accuracy in Mobile Environments

Mobility in wireless networks is characterized by the presence of doppler shift in transmissions over the channel. The comparative performance of Aileron with respect to the different input modulations in a mobile environment is similar to that described in Section 5.2, albeit with different accuracy values.

Fig. 13 shows the lowest SNR at which active-mode Aileron can achieve 90 percent accuracy for BPSK, QPSK and 8 PSK modulations under different mobility speeds. The accuracy of Aileron is computed using 50,000 AMR windows, each with a length of 50. In this environment,

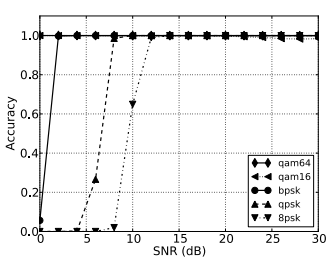

Fig. 12. Passive-mode Aileron accuracy in a simulated channel with no doppler shift and an AMR window of 20.

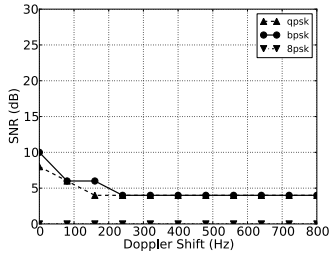

Fig. 13. Lowest SNR level at which the accuracy of active-mode Aileron exceeds 90 percent, using an AMR window of 50.

BPSK and QPSK modulations can be correctly identified 90 percent of the time at SNR greater than 10 and 7 dB, respectively, while greater than 90 percent accuracy in recognizing 8 PSK is achieved for all the considered SNR levels and doppler shifts.

Fig. 14 shows the results of minimum SNR at which passive mode Aileron can achieve 90 percent accuracy. We use an AMR window size of 10. At SNR greater than 12 dB, BPSK and QPSK can be correctly recognized with 90 percent, while at 22 dB SNR and above, 8 PSK can be recognized with 90 percent accuracy with a doppler frequency of up to 800 Hz.

6 Evaluation Using Real Channels

6.1 Experimental Setup

We evaluate the accuracy of modulation-based signaling using USRP2 devices deployed over eight locations of a single floor of our department building. The GNURadio implementation of modulation-based signaling from Section 5 with the parameters in Table 1 is used in these experiments. A trace collection proceeds as follows. A transmitter is placed at one of the eight locations and it transmits approximately 10,000 frames using five randomly-selected OFDMA subchannels. All five modulation rates are simultaneously used to transmit a frame. The nodes placed at the other seven locations receive and decode this transmission. Each transmitter repeats the 10,000-frame transmission 10 times, with a different set of five subchannels selected each time.

This collection procedure is performed at each of the eight node positions to collect a total of approximately 100 million OFDMA blocks. Since the traces are collected during normal working hours, the recorded channel conditions include environmental mobility effects due to the movements of people around the office floor. In the rest of this section, we will present the accuracy of Aileron based on these traces with an AMR window of size 10.

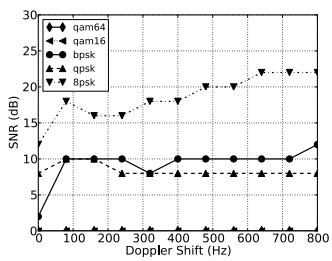

Fig. 14. Lowest SNR level at which accuracy of active-mode Aileron exceeds 90 percent, using an AMR window of 10.

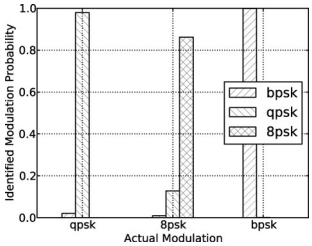

Fig. 15. Active-mode Aileron accuracy over the good-quality channel.

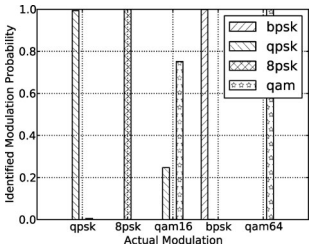

Fig. 16. Passive-mode Aileron accuracy over the good-quality channel.

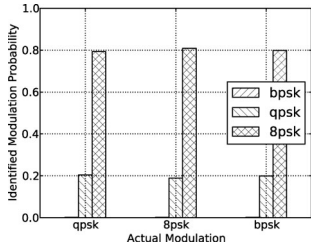

Fig. 18. Active-mode Aileron accuracy over the poor-quality channel.

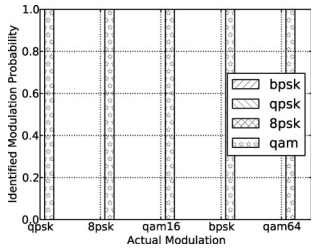

Fig. 19. Passive-mode Aileron accuracy over the poor-quality channel.

6.2 Channel SNR Characteristics

SNR for each subchannel is computed only for every AMR window using only the PSK-modulated subcarriers as these have a known transmission magnitude. The received signal energy is estimated using the mean magnitude of the received PSK symbols while the noise power is estimated using the variance of this magnitude over the AMR window. The ratio of this estimated signal-to-noise power is the SNR of the subchannel and is presented here in decibels (dB).

Fig. 17a shows that the distribution of the overall SNR of all non-overlapping AMR windows across all point-to-point links varies over a wide range, from 5 to 32 dB. 18 percent of the AMR windows have SNRs between 5 and 7 dB while 60 percent have SNRs between 23 and 32 dB. The remaining 22 percent of the AMR windows have SNRs between 7 and 23 dB. The SNR distribution of each link can differ significantly from that shown in Fig. 17a. To illustrate the performance of Aileron across a wide range of channel conditions, we focus on traces from three channels with distinctly different SNR distributions: poor, intermediate and good quality channels. The SNR distributions of these three channels are plotted in Figs. 17b, 17c and 17d, respectively.

6.3 Aileron Performance under Varying SNR

Under the high-SNR channel, active-mode Aileronis very accurate, as shown in Fig. 15. BPSK, QPSK and 8 PSK are correctly recognized with a probability of 100, 98 and 86 percent, respectively. This matches the performance of Aileronunder a simulated channel, as shown in Fig. 8. Note that this level of accuracy is achieved using an AMR window size of 10 under realistic conditions with environmental mobility. This shows that in high-SNR channels, modulation-based signaling with Aileron is reliable and feasible for low rate coordination purposes.

Fig. 16 shows the performance of passive-mode Aileron with data subcarriers in the good channel. For each modulation rate transmitted over this subchannel, we plot the probability of it being detected as "BPSK", "QPSK", "8 PSK" or "QAM" by the AMR as described in Algorithm 1. Under the high-SNR channel, BPSK, QPSK, 8 PSK and 64 QAM modulation schemes in the data subcarriers are detected with 100 percent accuracy. 16 QAM, on the other hand, is only correctly identified 75 percent of the time. Again, this matches the results obtained using the emulated channel as shown in Fig. 11.

The SNR of the poor-quality channel varies between 5 and 9 dB. At such low SNRs, both active and passive mode Aileron have low accuracy, as shown in Figs. 18 and 19. This is consistent with the results in Figs. 8 and 11 that are obtained over the simulated channel. However, note that passive-mode Aileron is not confused between the different decision rules and returns the default "QAM" result in every case where it cannot correctly identify the modulation scheme used.

With an intermediate quality channel, we can see from Fig. 17c that up to 38 percent of the SNR values are below 10 dB while at least 40 percent of the SNR experienced is above 25 dB. Under such mixed conditions, active-mode Aileron can correctly recognize BPSK, QPSK, and 8 PSK

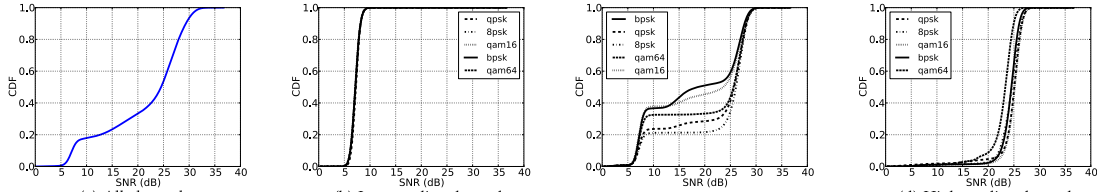

(a) All channels (b) Low quality channel (c) Intermediate quality channel (d) High quality channel

Fig. 17. SNR of channels encountered during experimental evaluations with the USRP.

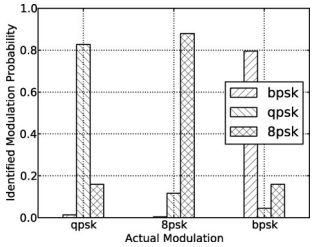

Fig. 20. Active-mode Aileron accuracy over the intermediate-quality channel.

with 80, 82 and 89 percent of the time, respectively as shown in Fig. 20. This demonstrates that modulation-based signaling is reliable over channels that experience highly variable SNR.

Passive-mode Aileron can also accurately determine the modulation rate in data subcarriers, as shown in Fig. 21. Notice that with data subcarriers, similar to the case of low-SNR channels, no PSK scheme is confused as another.

7 Discussion

7.1 Increasing Detection Accuracy

Both our simulated and real-world experiments are designed to closely match the capabilities of our USRP configuration. As a result, all signals are processed at the Nyquist rate. In practical implementations of Aileron, *oversampling* can be used to improve its detection accuracy significantly. An oversampling factor of k means that the data frame is received at k times its Nyquist bandwidth.

Fig. 23 shows how the root-mean-squared Error Vector Magnitude (EVM) of symbols in 20 MHz 802.11a frames varies when different oversampling factors are used. At each modulation rate, the EVM is computed over 10,000 802.11a frames that are transmitted over a `jtcInOffC` channel.

The EVM of the received signals decreases with increasing oversampling factors and we can expect a similar detection improvement in Aileron with oversampling. Oversampling is a technique widely employed by commercial wireless devices and can thus be easily integrated into Aileron.

7.2 Rate-Delay Tradeoff

Aileron is used to concurrently send control information to receivers that are otherwise unable to decode the primary transmission. For example, an AP in a multi-channel WLAN can concurrently send ACK and data frames to two WLAN clients that are on different channels. However, encoding information using modulation rates can cause the data frame to be transmitted at a sub-optimal rate. Even so, this data-rate reduction compensated by a significant

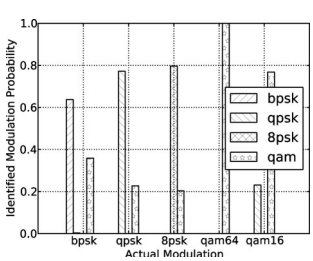

Fig. 21. Passive-mode Aileron accuracy over the intermediate-quality channel.

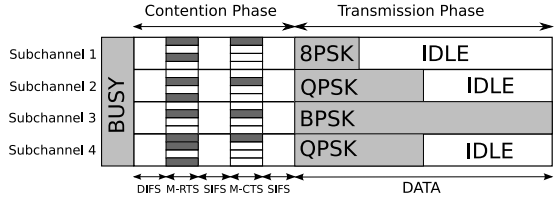

Fig. 22. Example channel utilization without Aileron.

reduction in the network coordination overhead due to the seamless exchange of Aileron control frames. In the multi-channel WLAN scenario, the median channel switching delay of 15 ms [11] is an order of magnitude larger than the data transmission time (less than 1 ms at 54 Mbps). This delay constitutes a significant overhead in typical multi-channel transmissions, especially with short packets such as ACKS. Aileron eliminates this coordination overhead when short control frames have to be sent to out-of-band receivers. We believe that this presents a beneficial rate-delay tradeoff when dealing with challenging wireless networks, such as multi-channel and cognitive radio networks.

7.3 Fading Channels

Modulation identification in Aileron is conducted over a window of OFDM symbols and the window size can be extended to neutralize the effects of channels with particularly long fading durations. Our choice of a 10-symbol window size is based on real-world measurements and has been shown to offer good performance over actual real-world fading channels.

Bit interleaving and channel coding are typically used to increase the resilience of 802.11 frames to the effects of channel fades. Such techniques are orthogonal to Aileron, which employs a predominantly PHY layer signaling mechanism. Cross-layer integration of these techniques, though possible, are beyond the scope of this paper.

8 Example: Improvement of Channel Utilization

Channelization of a wideband spectrum [1], [12] is a well-known approach to improving the utilization of a wireless channel. FICA [1] is an example PHY that adopts channelization and frequency domain contention [13], [14], [15] to improve wireless channel utilization. However, a key limitation of FICA comes from the fact that after each contention round, only a fixed, predefined number of OFDM symbols can be transmitted on each subchannel. This is to ensure that each wireless node occupies a constant amount of airtime, regardless of the modulation rate

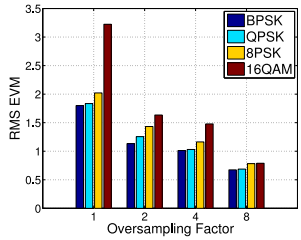

Fig. 23. EVM of symbols in a 20 MHz 802.11a frame at different modulation rates

used. Obviously, this approach can be limiting for traffic that is bursty or consists of a large range of frame size, as is the case with interactive web traffic and multimedia streaming applications. We note that frame aggregation is orthogonal, yet complementary to channelization. Channelization increases the number of concurrent transmitters, but the bandwidth available to each transmitter at any time is stochastic in nature. On the other hand, frame aggregation gives the transmitter the flexibility to maximize the use of its available bandwidth.

In this section, we demonstrate how Aileron can be used to replace the fixed transmission portion of FICA with one that allows each node to transmit a variable number of frames. We dynamically determine the number of aggregated frames to be transmitted by each node from the relative modulation rates of the other concurrent transmitters, but without any explicit coordination between any pair of nodes. This mechanism is simple but can be easily extended to encompass more complex aggregation protocols. We leave such exploration as future work.

8.1 Protocol Description

FICA divides the wireless channel into multiple non-overlapping subchannels. Each subchannel has a set of subcarriers, known as the *contention band*, that is used for channel contention.

Actual channel use is separated into the contention phase and the transmission phase, and progress from one phase to the other is time-synchronized across all clients. When the entire channel is sensed to be idle for a length of time equal to the DIFS, each client sends a frequency-domain Binary Amplitude Modulation (BAM) signal on a randomly-selected contention band. The AP then waits for a further SIFS-specified duration before picking a winning subcarrier in each contention band. It sends a BAM ACK signal on the winning contention bands and the clients associated with those bands then proceed with data transmissions.

Two key observations can be made here. First, during channel contention, the AP does not know the ID of any contending client. Second, at the end of the channel contention, each client only knows if it has won access to its selected channels. Clients do not know the winner of any other non-selected subchannel or of any selected channel that it fails to win access to.

Before describing our extension to FICA, we make the following assumptions. First, a fixed number of subcarriers, known as *control subcarriers*, at known positions in each subchannel are used by active-mode Aileron to encode the address of the transmitting client. Second, the modulation rate of the remaining subcarriers are selected by a rate-control algorithm. Third, all data frames are of the same length 1.5 KB, which is typically the case for bulk data transfer scenarios. Finally, different subchannels can use different modulation rates, but all data subcarriers in the same subchannel must use the same modulation rate.

Under these assumptions, if the capability to transmit multiple frames is not available, the channel utilization will resemble the illustration in Fig. 22. The "good" quality subchannels that can transmit frames at higher bit-rates will suffer from lower utilization. With Aileron, clients can opportunistically transmit additional frames during these idle periods while maintaining the high channel utilization of FICA. We combine the channel contention phase of FICA with a transmit scheduling algorithm, shown in Algorithm 2, that uses Aileron.

Algorithm 2. Search for Transmission Opportunities

Input: $\mathcal{N}$ is the set of all active nodes in the current transmission phase; $\mathcal{C}$ is the set of all subchannels; P is the size of each transmitted frame; k is the ID of the node executing this search algorithm; C_n is the set of channels assigned to node $n \in \mathcal{N} \setminus \{k\}$; R_c is the transmission rate of each channel $c \in \mathcal{C}$; M_k is the total number of frames sent in the current transmission phase.

```
begin
  T[k] ← P/∑_{c∈C_k} R_c;
  for n ∈ N \ {k} do
      r ← ∑_{c∈C_n} R_c;
      T[n] ← P/r;
  end
  m ← max_{n∈N\{k}} T[n];
  if m − T[k] · (M_k + 1) ≥ T[k] then
      M_k ← M_k + 1;
      Schedule another frame for transmission;
  else
      M_k ← 0;
      Wait for the next contention phase;
  end
end
```

Let $\mathcal{N}$ be the set of Aileron clients and C_n be the channels assigned to each client $n \in \mathcal{N}$ for the current data transmission phase. During the data transmission phase, each node encodes its ID in the predefined subcarriers within its assigned subchannels. When a node k completes its transmission, it enters the idle state. It listens for N OFDM blocks on each subchannel and uses passive Aileron to determine the modulation rate of each subchannel. The node k also determines the set of channels in use by each neighbor, C_n for $n \in \mathcal{N} \setminus \{k\}$, from the IDs encoded in the control subcarriers. Full duplex wireless communications [16] can be used to collect these N OFDM blocks concurrently with the transmission to minimize the overhead of Aileron.

With these two pieces of information, the node can determine the transmission time required by each neighbor and the remaining transmission duration of the slowest node. Note that the transmission time in use by a node depends on both the rate used in each of its subchannels and the total number of subchannels assigned to it. Let M_k be the total number of frames sent by node k in the current transmission phase. If the channel occupancy of the slowest node is greater than the time required for node k to transmit $M_k + 1$ frames, then an additional frame is sent within this remaining duration using its assigned subchannels. Otherwise, it simply waits for the next transmission round.

8.2 Simulation Setup

We demonstrate the improvements achieved by Aileron in FICA using a custom simulator that models the Aileron performance in detail. In our simulation, we evaluate

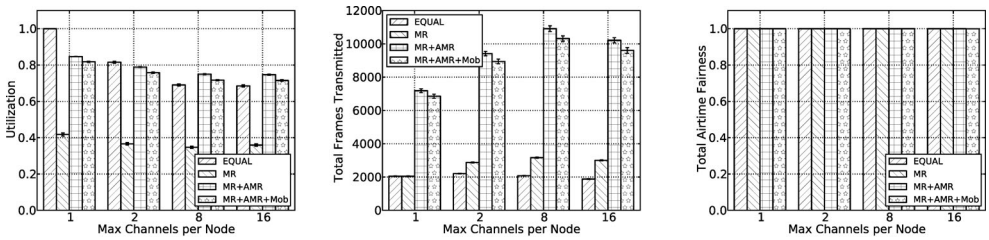

(a) Channel utilization (b) Total number of frames transmitted (c) Throughput fairness

Fig. 24. Mean and standard deviation of the three evaluation metrics. The mean is represented by the height of the bar while the error bars indicate the standard deviation.

Aileron using the same PHY and channel parameters as shown in Tables 1 and 2, except that we limit the size of the AMR window to 10, 15, 20 and 25 blocks. FICA utilizes two frequency backoff policies, AIMD and RMAX, but we only present results that use RMAX as it has been shown in [1] to outperform AIMD. All the SNR values between every pair of nodes and between each node on the AP are governed by identical and independently distributed random variables that follow the distribution shown in Fig. 17a. The modulation detection accuracy at various SNR and doppler shift values follow the simulated results described in Section 5.

Each simulation run consists of a single AP and 10 contending FICA clients. We run the simulation for 1,000,000 time units, where a single time unit is equivalent to the transmission time of a single OFDM block. The results shown here are obtained from 20 simulation repetitions.

In our evaluation, we do not explicitly model the effects of an auto-rate algorithm. Instead, given the SNR of the channel, we simply pick the highest modulation rate from the known bit error rate (BER) graph [17] that can meet a maximum BER of 10^{-4}.

The three performance metrics that we use are:

M1. Per-Node channel utilization. This is the ratio of the total transmission time of a node during a single transmission phase to the duration of the entire transmission phase. The duration of the transmission phase is lower-bounded by the slowest transmitting rate among all the active nodes.

M2. Airtime fairness. We use the Jain's fairness index to determine how the channel is shared among the competing nodes. Since the channel access time of every node is affected by its utilization, this essentially illustrates how the channel utilization varies across the Aileron nodes.

M3. Total frames transmitted. This is a simple count of the total number of frames that are transmitted over the duration of the simulation and is a measure of the throughput.

The four scenarios considered in our simulations are:

S1. Equal rate (EQUAL). All clients transmit with the same modulation rate during each transmission phase. This rate is chosen such that a BER of at most 10^{-4} is achieved on the channel with the lowest SNR.

S2. Multi rate (MR). During each transmission phase, the highest modulation rate on each channel, with respect to the SNR, that can achieve a BER of at most 10^{-4} is chosen.

S3. Multi rate with AMR (MR+AMR). This is similar to MR, except that Aileron is now used to find transmission opportunities for nodes with high transmission rates.

S4. Multi rate with AMR and mobility (MR + AMR + Mob). This is MR+AMR with the addition of mobile nodes. Node velocities are randomly assigned and are characterized by the presence of doppler shift in the channel.

Aileron is not used in EQUAL and MR. Hence, only one frame is sent in each transmission opportunity in EQUAL and MR.

8.3 Simulation Results

For brevity, we only show the results obtained with an AMR window of 10 since the results obtained with larger AMR window sizes show similar behavior. Fig. 24a shows the mean and standard deviation of the channel utilization of EQUAL, MR, AMR+MR and AMR+MR+Mob with different numbers of maximum channels per node.

Observe that EQUAL with only one channel per node achieves maximum utilization of the channel, since all frames are transmitted at the same rate and the channel is never idle. However, when each transmitter under the EQUAL scenario is allowed to contend for more than one channel, channel utilization drops from 82 percent with up to two channels per node, to 70 percent when each node can contend for all 16 channels. Varying the number of channels per node effectively varies the throughput by each node. The resulting idle periods belonging to nodes with high throughput reduces overall channel utilization. This effect of heterogeneous throughput on channel utilization is even more dramatic when the modulation rates of different subchannels are allowed to vary under the MR scenario—mean channel utilization drops to under 40 percent, regardless of the number of allowable channels per node.

Aileron can improve the channel utilization by opportunistically sending a frame if sufficient time remains before the slowest node completes its transmission. With up to two channels per node in the MR+AMR scenario, Aileron can achieve 79 percent channel utilization. When each node can contend for all channels, Aileron achieves 76 percent channel utilization, which is above that achieved in the EQUAL scenario. This significant improvement in channel utilization is present even with node mobility.

Besides the improvement in channel utilization, Aileron also increases the mean throughput of each node, as shown by the count of transmitted shown in Fig. 24b. When all nodes are limited to only one channel, there is no throughput difference between the EQUAL and MR scenarios since high throughput nodes in MR are still limited by the low throughput nodes. When the number of allowable channels increases, nodes in the MR scenario have a higher throughput than those in the EQUAL scenario. This reflects

the advantage of a per-channel modulation rate adaptation. Aileron is able to significantly increase the achievable throughput via appropriate opportunistic transmissions. When the clients can contend for up to eight channels, almost 11,000 frames are transmitted on average using Aileron while only 2,000 and 3,000 frames are transmitted in the EQUAL and MR scenarios, respectively. This throughput increase achieved by Aileron does not come at the expense of throughput fairness among the transmitting nodes, as shown in Fig. 24c.

9 Related Work

Control channel design. Typical control channels can be classified to be in-band or out-of-band. In-band control channels carry control frames in the same channel as that used for data frames. Examples include in-band medium access control using CSMA [18] and slotted ALOHA [19]; probe frames for auto-rate selection [20]; link-quality measurements in mesh networks [21]; transmitting control frames using side-channels [22] and inter-frame gaps [23]. SMACK [24] extends the in-band control to the PHY layer through its use of on-off OFDM subcarrier signaling for sending acknowledgements. 802.11ec [25] uses known correlation sequences along with a shared dictionary to convey predetermined messages. Out-of-band approaches are characterized by the use of a dedicated channel for control frames. If only one wireless interface is available [26], the need for it to be switched between the control and data channels incurs a significant coordination overhead. If multiple interfaces are available [27], the coordination overhead is reduced at the cost of higher hardware and power requirements.

Modulation recognition. The method of modulation recognition in [28] is based on the differences of MSE, but its recognition algorithm is too simplistic to be able to differentiate PSK from QAM modulations. Other recognition methods include the use of higher-order statistics [29], wavelet transform [30], and cyclic features of the digital transmission [31].

10 Conclusion

In this paper, we have presented Aileron, a novel design for control channel in OFDM(A) wireless networks. It is a new paradigm of communications which uses the *modulation type*, rather than the *symbol value*, to encode information. It is built upon the concept of AMR and supports two modes of operation: (a) *active* mode, where ternary-valued control frames are sent over subcarriers, and (b) *passive* mode, where the modulation rate of data subcarriers is automatically detected. We have evaluated Aileron using both simulated and real-world channels to demonstrate both its feasibility and reliability. We have also integrated Aileron into FICA and showed how throughput and channel utilization can be improved with frame aggregation in dynamic spectrum networks.

Acknowledgments

The work reported in this paper was supported in part by the US National Science Foundation under grants CNS-1160775 and CNS-1317411. E. Chai is the corresponding author.

References

[1] K. Tan, J. Fang, Y. Zhang, S. Chen, L. Shi, and J. Zhang, "Fine-grained channel access in wireless LAN," in *Proc. ACM SIGCOMM Conf.*, 2010, pp. 147–158.

[2] K. Bian, J.-M. Park, and R. Chen, "A quorum-based framework for establishing control channels in dynamic spectrum access networks," in *Proc. 15th Annu. Int. Conf. Mobile Comput. Netw.*, 2009, pp. 25–36.

[3] Y. Yuan, P. Bahl, R. Chandra, P. A. Chou, I. Ferrell, T. Moscibroda, S. Narlanka, and Y. Wu, "Knows: Kognitiv networking over white spaces," in *Proc. IEEE Dynam. Spectrum Access Netw.*, 2007, pp. 416–427.

[4] M. Pedzisz and A. Mansour, "Automatic modulation recognition of MPSK signals using constellation rotation and its 4th order cumulant," *Digital Signal Process.*, vol. 15, pp. 295–304, May 2005.

[5] A. Nandi and E. E. Azzouz, "Algorithms for automatic modulation recognition of communication signals," *IEEE Trans. Commun.*, vol. 46, no. 4, pp. 431–436, Apr. 1998.

[6] D. Halperin, W. Hu, A. Sheth, and D. Wetherall, "Predictable 802.11 packet delivery from wireless channel measurements," in *Proc. ACM SIGCOMM Conf.*, 2010, pp. 159–170.

[7] M. Vutukuru, K. Jamieson, and H. Balakrishnan, "Harnessing exposed terminals in wireless networks," in *Proc. 5th USENIX Symp. Netw. Syst. Des. Implementation*, 2008, pp. 59–72.

[8] S. Rayanchu, V. Shrivastava, S. Banerjee, and R. Chandra, "FLUID: Improving throughputs in enterprise wireless LANs through flexible channelization," in *Proc. 17th Annu. Int. Conf. Mobile Comput. Netw.*, 2011, pp. 1–12.

[9] O. Dobre, A. Abdi, Y. Bar-Ness, and W. Su, "Survey of automatic modulation classification techniques: Classical approaches and new trends," *Commun., IET*, vol. 1, no. 2, pp. 137–156, 2007.

[10] J. van de Beek, M. Sandell, and P. Borjesson, "ML estimation of time and frequency offset in OFDM systems," *IEEE Trans. Signal Process.*, vol. 45, no. 7, pp. 1800–1805, Jul. 1997.

[11] R. Chandra, R. Mahajan, T. Moscibroda, R. Raghavendra, and P. Bahl, "A case for adapting channel width in wireless networks," in *Proc. ACM SIGCOMM Conf. Data Commun.*, 2008, pp. 135–146.

[12] L. Yang, W. Hou, L. Cao, B. Zhao, and H. Zheng, "Supporting demanding wireless applications with frequency-agile radios," in *Proc. 7th USENIX Conf. Netw. Syst. Des. Implementation*, 2010, p. 5.

[13] Y.-J. Chang, F.-T. Chien, and C. Kuo, "Opportunistic access with random subchannel backoff (OARSB) for OFDMA uplink," in *Proc. IEEE Global Telecommun. Conf.*, 2007, pp. 3240–3244.

[14] B. Roman, F. Stajano, I. Wassell, and D. Cottingham, "Multi-carrier burst contention (MCBC): Scalable medium access control for wireless networks," in *Proc. IEEE Wireless Commun. Netw. Conf.*, 2008, pp. 1667–1672.

[15] B. Roman and I. Chatzigeorgiou, "Evaluation of multi-carrier burst contention and IEEE 802.11 with fading during channel sensing," in *Proc. IEEE 20th Int. Symp. Personal, Indoor Mobile Radio Commun.*, 2009, pp. 57–61.

[16] M. Jain, J. Choi, T. Kim, D. Bharadia, S. Seth, K. Srinivasan, P. Levis, S. Katti, and P. Sinha, "Practical, real-time, full duplex wireless," in *Proc. 17th Annu. Int. Conf. Mobile Comput. Netw.*, 2011, pp. 301–312.

[17] J. Proakis, *Digital Communications*, 4th ed. New York, NY, USA: McGraw-Hill.

[18] A. Woo and D. E. Culler, "A transmission control scheme for media access in sensor networks," in *Proc. 7th Annu. Int. Conf. Mobile Comput. Netw.*, 2001, pp. 221–235.

[19] L. G. Roberts, "ALOHA packet system with and without slots and capture," in *Proc. ACM SIGCOMM Comput. Commun. Rev.*, Apr. 1975, pp. 28–42.

[20] H. Rahul, F. Edalat, D. Katabi, and C. Sodini, "Frequency-aware rate adaptation and MAC protocols," in *Proc. 15th Annu. Int. Conf. Mobile Comput. Netw.*, 2009, pp. 193–204.

[21] K. H. Kim and K. G. Shin, "On accurate and asymmetry-aware measurement of link quality in wireless mesh networks," *IEEE/ACM Trans. Netw.*, vol. 17, no. 4, pp. 1172–1185, Aug. 2009.

[22] K. Wu, H. Tan, Y. Liu, J. Zhang, Q. Zhang, and L. Ni, "Side channel: Bits over interference," in *Proc. 16th Annu. Int. Conf. Mobile Comput. Netw.*, 2010, pp. 13–24.

[23] K. Chebrolu and A. Dhekne, "Esense: Communication through energy sensing," in *Proc. 15th Annu. Int. Conf. Mobile Comput. Netw.*, 2009, pp. 85–96.

[24] A. Dutta, D. Saha, D. Grunwald, and D. Sicker, "SMACK: A SMart ACKnowledgment scheme for broadcast messages in wireless networks," *ACM SIGCOMM Comput. Commun. Rev.*, vol. 39, pp. 15–26, Oct. 2009.
[25] E. Magistretti, O. Gurewitz, and E. W. Knightly, "802.11ec: Collision avoidance without control messages," in *Proc. 18th Annu. Int. Conf. Mobile Comput. Netw.*, 2012, pp. 65–76.
[26] J. So and N. Vaidya, "Multi-channel MAC for ad hoc networks: Handling multi-channel hidden terminals using a single transc eiver," in *Proc. 5th ACM Int. Symp. Mobile Ad Hoc Netw. Comput.*, 2004, pp. 222–233.
[27] J. Wang, Y. Fang, and D. Wu, "A power-saving multi-radio multi-channel MAC protocol for wireless local area networks," in *Proc. 25th IEEE Int. Conf. Comput. Commun.*, 2006, pp. 1–12.
[28] M. Naik, A. Mahanta, R. Bhattacharjee, and H. B. Nemade, "An Automatic blind modulation recognition algorithm for M-PSK signals based on MSE criterion," *E-Bus. Telecommun. Netw., Commun. Comput. Inf. Sci.*, vol. 3, pp. 257–266, 2007.
[29] A. Swami and B. Sadler, "Hierarchical digital modulation classification using cumulants," *IEEE Trans. Commun.*, vol. 48, no. 3, pp. 416–429, Mar. 2000.
[30] K. Ho, W. Prokopiw, and Y. Chan, "Modulation identification of digital signals by the wavelet transform," *IEE Proc. Radar, Sonar Navigation*, vol. 147, no. 4, pp. 169–176, Aug. 2000.
[31] B. Ramkumar, "Automatic modulation classification for cognitive radios using cyclic feature detection," *IEEE Circuits Syst. Mag.*, vol. 9, no. 2, pp. 27–45, Jun. 2009.

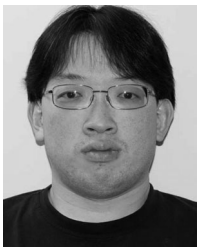

Eugene Chai received the MSE degree in 2009 and the PhD degree in 2013, from the Computer Science and Engineering Department at the University of Michigan, Ann Arbor, under the guidance of Professor Kang G. Shin. He is a researcher at NEC Laboratories America in Princeton, NJ. His research interests lie in the design and implementation of next-generation LTE networks. He is the member of the IEEE.

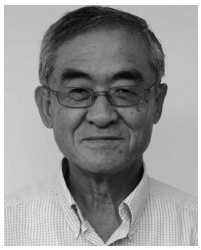

Kang G. Shin is the Kevin & Nancy O'Connor professor of computer science in the Department of Electrical Engineering and Computer Science, The University of Michigan, Ann Arbor. His current research focuses on QoS-sensitive computing and networking as well as on embedded real-time and cyber-physical systems. He has supervised the completion of 75 PhDs, and authored/coauthored more than 830 technical articles, one textbook and more than 30 patents or invention disclosures, and received numerous best paper awards, including the Best Paper Awards from the 2011 ACM International Conference on Mobile Computing and Networking (MobiCom11), the 2011 IEEE International Conference on Autonomic Computing, the 2010 and 2000 USENIX Annual Technical Conferences, as well as the 2003 IEEE Communications Society William R. Bennett Prize Paper Award and the 1987 Outstanding IEEE Transactions of Automatic Control Paper Award. He has also received several institutional awards, including the Research Excellence Award in 1989, Outstanding Achievement Award in 1999, Distinguished Faculty Achievement Award in 2001, and Stephen Attwood Award in 2004 from The University of Michigan (the highest honor bestowed to Michigan Engineering faculty); a Distinguished Alumni Award of the College of Engineering, Seoul National University in 2002; 2003 IEEE RTC Technical Achievement Award; and 2006 Ho-Am Prize in Engineering (the highest honor bestowed to Korean-origin engineers). He has chaired several major conferences, including 2009 ACM MobiCom, 2008 IEEE SECON, 2005 ACM/USENIX MobiSys, 2000 IEEE RTAS, and 1987 IEEE RTSS. He has served on editorial boards, including *IEEE Transactions on Parallel and Distributed Systems* and *ACM Transactions on Embedded Systems*. He has also served or is serving on numerous government committees, such as the US NSF Cyber-Physical Systems Executive Committee and the Korean Government R&D Strategy Advisory Committee. He has also co-founded a couple of startups. He is the fellow of the IEEE and ACM.